Hydroxyl Radical Formation during Peroxynitrous Acid Decomposition

John W. Coddington,[†] James K. Hurst,*[,†] and Sergei V. Lymar[‡]

Contribution from the Departments of Chemistry, Washington State University, Pullman, Washington 99164-4630, and Brookhaven National Laboratory, Upton, New York 11973-5000

Received August 11, 1998

Abstract: Yields of O_2 formed during decomposition of peroxynitrous acid (ONOOH) under widely varying medium conditions are compared to predictions based upon the assumption that the reaction involves formation of discrete $^{\bullet}OH$ and $^{\bullet}NO_2$ radicals as oxidizing intermediates. The kinetic model used includes all reactions of $^{\bullet}OH$, $^{\bullet}O_2^-$, and reactive nitrogen species known to be important under the prevailing conditions; because the rate constants for all of these reactions have been independently measured, the calculations contain no adjustable fitting parameters. The model quantitatively accounts for (1) the complex pH dependence of the O_2 yields and (2) the unusual effects of NO_2^-, which inhibits O_2 formation in neutral, but not alkaline, solutions and also reverses inhibition by organic $^{\bullet}OH$ scavengers in alkaline media. Other observations, including quenching of O_2 yields by ferrocyanide and bicarbonate, the pressure dependence of the decomposition rate, and the reported dynamic behavior for O_2 generation in the presence of H_2O_2, also appear to be in accord with the suggested mechanism. Overall, the close correspondence between observed and calculated O_2 yields provides strong support for decomposition via homolysis of the ONOOH peroxo bond.

Introduction

Peroxynitrite ion ($ONOO^-$) and its conjugate acid (ONOOH) are powerful oxidants whose chemistry is presently poorly understood.[1−3] Although regarded historically as laboratory curiosities, there is mounting circumstantial evidence that peroxynitrite and its derivatives may play major roles in cellular defense mechanisms against microbial infection[4−7] and the pathophysiology of human diseases associated with oxidative stress.[8] Consequently, within the past few years there has been an explosion of interest in conditions that promote peroxynitrite formation and its subsequent reactivity.[9]

The peroxynitrite anion is relatively unreactive, presumably because its reduction generates O^{2-} as a leaving group.[10] However, protonation[1] or addition of other Lewis acids (e.g., CO_2[11−13] or complexation by certain metal ions[14,15]) generates reactive species which either oxidize compounds present in the medium or undergo rapid degradation, leading to net isomerization to NO_3^- ion.[1,16] Both one-electron and two-electron oxidations have been observed.[3] The one-electron reactions often proceed by rate-limiting unimolecular activation of ONOOH (or $ONOOCO_2^-$), for which maximal product yields obtained are always substantially less than limits based upon stoichiometric consumption of the oxidant.[16−22] This behavior indicates the existence of at least two intermediates along the reaction pathway, only one of which is oxidizing but both of which are capable of forming NO_3^-.[2,3,16−22] In contrast, two-electron oxidations appear to involve direct bimolecular reaction between ONOOH and the reductant.[3,18,23−26]

* Address correspondence to this author. E-mail: hurst@wsu.edu. FAX: (509) 335-8867.

[†] Washington State University.

[‡] Brookhaven National Laboratory.

(1) Edwards, J. O.; Plumb, R. C. *Prog. Inorg. Chem.* **1994**, *41*, 599−635.

(2) Koppenol, W. H.; Moreno, J. J.; Pryor, W. A.; Ischiropoulos, H.; Beckman, J. S. *Chem. Res. Toxicol.* **1992**, *5*, 834−842.

(3) Pryor, W. A.; Squadrito, G. L. *Am. J. Physiol.* **1995**, *268*, L699−L722.

(4) Evans, T. J.; Buttery, L. D. K.; Carpenter, A.; Springall, D. R.; Polak, J. M.; Cohen, J. *Proc. Natl. Acad. Sci. U.S.A.* **1996**, *93*, 9553−9558.

(5) Hurst, J. K.; Lymar, S. V. *Acc. Chem. Res.* In press.

(6) Denis, M. *J. Leuk. Biol.* **1994**, *55*, 682−684.

(7) Kuhl, S. J.; Rosen, H. *Curr. Opin. Infect. Dis.* **1995**, *8*, 181−185.

(8) Beckman, J. S.; Koppenol, W. H. *Am. J. Physiol. Cell Physiol.* **1996**, *271*, C1424−C1437 and references therein.

(9) Various viewpoints have been summarized in invited papers published collectively as a discussion forum in: *Chem. Res. Toxicol.* **1998**, *11*, 709−721.

(10) Lymar, S. V.; Hurst, J. K. *Chem. Res. Toxicol.* **1998**, *11*, 714−715.

(11) Lymar, S. V.; Hurst, J. K. *J. Am. Chem. Soc.* **1995**, *117*, 8867−8868.

(12) Uppu, R. M.; Squadrito, G. L.; Pryor, W. A. *Arch. Biochem. Biophys.* **1996**, *327*, 335−343.

(13) Denicola, A.; Freeman, B. A.; Trujillo, M.; Radi, R. *Arch. Biochem. Biophys.* **1996**, *333*, 49−58.

(14) Groves, J. T.; Marla, S. S. *J. Am. Chem. Soc.* **1995**, *117*, 9578−9579.

(15) Stern, M. K.; Jensen, M. P.; Kramer, K. *J. Am. Chem. Soc.* **1996**, *118*, 8735−8736.

(16) Lymar, S. V.; Hurst, J. K. *Inorg. Chem.* **1998**, *37*, 294−301.

(17) Lymar, S. V.; Jiang, Q.; Hurst, J. K. *Biochemistry* **1996**, *35*, 7855−7861.

(18) Goldstein, S.; Czapski, G. *Inorg. Chem.* **1995**, *34*, 4041−4048.

(19) Goldstein, S.; Czapski, G. *Inorg. Chem.* **1997**, *36*, 5113−5117.

(20) Crow, J. P.; Spruell, C.; Chen, J.; Gunn, C.; Ischiropoulos, H.; Tsai, M.; Smith, C. D.; Radi, R.; Koppenol, W. H.; Beckman, J. S. *Free Radical Biol. Med.* **1994**, *16*, 331−338.

(21) Goldstein, S.; Squadrito, G. L.; Pryor, W. A.; Czapski, G. *Free Radical Biol. Med.* **1996**, *21*, 965−974.

(22) Beckman, J. S.; Beckman, T. W.; Chen, J.; Marshall, P. A.; Freeman, B. A. *Proc. Natl. Acad. Sci. U.S.A.* **1990**, *87*, 1620−1624.

(23) Radi, R.; Beckman, J. S.; Bush, K. M.; Freeman, B. A. *J. Biol. Chem.* **1991**, *266*, 4244−4250.

(24) Pryor, W. A.; Jin, X.; Squadrito, G. L. *Proc. Natl. Acad. Sci. U.S.A.* **1994**, *91*, 11173−11177.

(25) Radi, R. *Chem. Res. Toxicol.* **1998**, *11*, 720−721.

(26) Goldstein, S.; Meyerstein, D.; van Eldik, R.; Czapski, G. *J. Phys. Chem. A* **1997**, *101*, 7114−7118.

10.1021/ja982887t CCC: $18.00
Published on Web 03/03/1999

Scheme 1

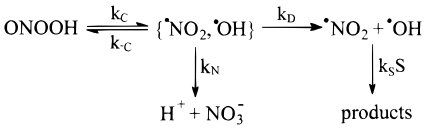

The structural basis for reactivity differences between intermediates formed from both ONOOH and $ONOOCO_2^-$ in the unimolecular (or "indirect") pathways has been the subject of considerable speculation. Reactivity has been assigned to specific configurational isomers (i.e., trans vs cis about the N−O single bond),[18,26] to high-energy "transoid" intermediates formed along reaction coordinates for cis−trans isomerization,[2] to nitronium (NO_2^+) ion (formed by heterolytic cleavage of the peroxo O−O bond),[3] and to caged radical pairs[3] or free radicals[16,27,28] (formed by homolytic cleavage of the O−O bond). We have recently emphasized that the reactivity patterns exhibited in simple one-electron "outer sphere" reactions with coordination compounds cannot be easily rationalized by dynamical models that impose high thermodynamic barriers to electron transfer to just one of the intermediates or by models based upon differing reactivities of geometrical isomers.[10] Since the peroxo O−O bond in these compounds is calculated to be exceptionally weak,[29] these facts are readily accommodated by a reaction model in which the "unreactive" intermediates are {$•NO_2$,•OH} and {$•NO_2$,$•CO_3^-$} caged radical pairs formed by O−O bond homolysis that either undergo rapid geminate recombination to form NO_3^- or escape the cage to give discrete radicals that engage in bimolecular reactions (Scheme 1).

For CO_2^-catalyzed reaction, it is generally agreed that formation of $•NO_2$ and $•CO_3^-$ from $ONOOCO_2^-$ is a plausible unimolecular activation step.[11,27,28,30] However, whether the rates of reactions of ONOOH are consistent with the thermodynamics of O−O bond homolysis to form $•NO_2$ and •OH is a contentious point.[9] In the present study, we compare product yields of O_2 formed by oxidation of $ONOO^-$ by the reactive intermediate under various conditions to values calculated assuming that the intermediate is •OH. These calculations are based upon a multistep radical mechanism that contains all of the reactions of •OH, $•O_2^-$, and reactive nitrogen species known to be important under the reaction conditions, including the recently reported reactions of •OH and N_2O_3 with $ONOO^-$,[31,32] and reversible dissociation of ONO_2^- to •NO and $•O_2^-$.[33] Because there are no adjustable parameters, the calculations provide a stringent test of the proposed mechanism. The comparison shows that reactivity of the oxidizing intermediate is indistinguishable from that of •OH; furthermore, the reaction scheme accurately accounts for the complex medium-dependent influence of NO_2^- and other •OH scavengers upon the system dynamics.

Experimental Section

Materials. All chemicals were reagent grade and used as received from commercial suppliers; water was purified with use of a Milli-Q system. Reagent solutions of sodium peroxynitrite were prepared from acidified H_2O_2 and $NaNO_2$ in a tandem quench-flow mixing apparatus[34] and stored at −80 °C. To minimize contamination of the stock solution by unreacted H_2O_2, $NaNO_2$ was taken in 10% stoichiometric excess. Analyses (described below) indicated that the product solution contained ~140 mM peroxynitrite, as determined spectrophotometrically (ϵ_{302} = 1670 M^{-1} cm^{-1}),[35] and 21 mM residual nitrite.

Analytical Methods. Rates and yields of oxygen production were measured with a Rank Brothers Clark type polarographic electrode system connected to a t−y strip-chart recorder. Experiments were performed at ambient temperature (21 ± 1 °C) by syringe-injecting aliquots of the alkaline peroxynitrite solution into a 5 mL cell containing rapidly stirred deoxygenated 0.3 M phosphate buffer. Oxygen yields were calculated from the magnitude of the change in polarographic current that accompanied complete decomposition of the peroxynitrite. Initial rates of O_2 formation measured at pH 9 were determined from the initial slopes of the current vs time traces; experimental conditions were adjusted so that the response of the O_2 electrode was not rate-limiting. The electrode was calibrated by reducing the O_2 in air-saturated water (0.279 mM O_2)[36] with solid sodium dithionite. Samples for nitrite and nitrate analyses were prepared by adding aliquots of the peroxynitrite stock solution to rapidly stirred phosphate buffer (pH 4−10). The nitrite ion content of the product solutions was determined by the Griess method.[36] The amount of residual nitrite ion present in the stock peroxynitrite solutions was determined by decomposing samples in phosphate buffer at pH 3, under which conditions nitrate is the sole nitrogen-containing product (Results section).[1,16] Nitrate ion was reduced to nitrite with *Aspergillus* nitrate reductase,[37] and determined as the difference in measured nitrite in the samples before and after enzymatic reduction.

Calculation Methods. The kinetics of peroxynitrite decay and oxygen formation were simulated by numerical integration of a set of rate equations with use of an INTKIN computer program developed by H. Schwarz at Brookhaven National Laboratory. The input parameters were initial concentrations of ONOOH, $ONOO^-$, and NO_2^-, medium pH, and pH-dependent rate constants for the reactions involved (Kinetic simulations section). The program generated temporal profiles for all reactants, intermediates, and products; the yields of O_2 were calculated as

$$\frac{[O_2]_{t\to\infty}}{([ONOOH] + [ONOO^-])_{t=0}}$$

Results

Reaction Stoichiometries. Two pathways have been identified for peroxynitrite decomposition in weakly acidic to alkaline solutions, one involving formation of nitrate:[1,16]

$$ONOOH \rightarrow H^+ + NO_3^- \qquad (1)$$

and the other, formation of nitrite and oxygen:[38]

$$ONOOH + ONOO^- \rightarrow O_2 + H^+ + 2NO_2^- \qquad (2)$$

As illustrated in Figure 1, the relative contribution of reaction 2 was insignificant below pH 4, rose steeply between pH 6.5 and 8.5, and approached a plateau value above pH 8.5. Under all conditions, the measured NO_2^-/O_2 ratio was nearly 2/1; this ratio was independent of the peroxynitrite concentration from 0.13 to 0.55 mM. Over the entire pH range studied, the O_2 yield was, within experimental uncertainties, independent of peroxynitrite concentrations over the range 0.14−0.55 mM. Furthermore, the total amount of NO_2^- plus NO_3^-, measured at pH 4,

(27) Merenyi, G.; Lind, J. *Chem. Res. Toxicol*. **1997**, *10*, 1216−1220.
(28) Goldstein, S.; Czapski, G. *J. Am. Chem. Soc*. **1998**, *120*, 3458−3463.
(29) Houk, K. N.; Condroski, K. R.; Pryor, W. A. *J. Am. Chem. Soc*. **1996**, *118*, 13002−13006.
(30) Koppenol, W. H.; Kissner, R. *Chem. Res. Toxicol*. **1998**, *11*, 87−90.
(31) Goldstein, S.; Saha, A.; Lymar, S. V.; Czapski, G. *J. Am. Chem. Soc*. **1998**, *120*, 5549−5554.
(32) Merenyi, G.; Czapski, G. Personal communication.
(33) Merenyi, G.; Lind, J. *Chem. Res. Toxicol*. **1998**, *11*, 243−246.
(34) Saha, A.; Goldstein, S.; Cabelli, D.; Czapski, G. *Free Radical. Biol. Med*. **1998**, *24*, 653−659.
(35) Hughes, M. N.; Nicklin, H. G. *J. Chem. Soc. A* **1968**, 450−452.
(36) Greenbert, A. E.; Conners, J. J.; Jenkins, D. *Standard Methods for the Examination of Water and Wastewater*, 15th ed.; American Public Health Association, United Book Press: Baltimore, 1995; pp *4*-83−*4*-84, *4*-99.
(37) Bories, P. N.; Bories, C. *Clin. Chem*. **1995**, *41*, 904−907.
(38) Pfeiffer, S.; Gorren, A. C. F.; Schmidt, K.; Werner, E. R.; Hansert, B.; Bohle, D. S.; Mayer, B. *J. Biol. Chem*. **1997**, *272*, 3465−3470.

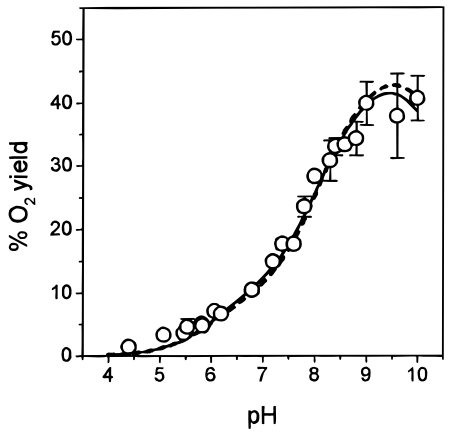

Figure 1. Experimental and calculated yields of O_2 formed during ONOOH decay. The solid line is the calculated yield assuming that reaction 3 forms NO_2^- and $^{\bullet}O_2^-$; the dashed line is the yield assuming that reaction 3 forms $^{\bullet}NO + O_2$. Error bars for experimental points are equal to twice the standard deviation of 12 (pH < 9) or 15 (pH ≥ 9) measurements for which the initial peroxynitrite concentration was varied from 0.13 to 0.55 mM in 0.3 M phosphate buffer.

Table 1. Oxygen Yield (%) for Selected Conditions of Added Nitrite and Radical Scavengers[a]

pH	[added NO_2^-] (mM)	[scavenger] (mM)	yield exp.[b]	yield calc.[c]
6.8	0	0	11 ± 0.5	10.8
6.8	0.20	0	8.9 ± 0.2	7.7
6.8	2.0	0	5.5 ± 0.2	4.0
6.8	40	0	2.6 ± 0.4	3.1
7.6	0	0	18 ± 0.5	19.0
7.6	1.0	0	13 ± 1	15.2
7.6	8.0	0	9.7 ± 0.7	14.0
7.6	40	0	9.6 ± 0.3	13.8
9.0	0	0	33 ± 1	39.7
9.0	1.0	0	32 ± 1	40.2
9.0	40	0	35 ± 2	40.3
9.0	400	0	33 ± 1	40.3
		$Fe(CN)_6^{4-}$		
9.0	0	0.50	8.1	4.8
9.0	0.5	0.50	8.8	3.7
9.0	5.0	0.50	9.2	2.9
9.0	0	5.0	1.6	0.7
9.0	5.0	5.0	1.6	0.7
		DMSO		
9.0	0	1.0	12 ± 3	
9.0	0.50	1.0	24 ± 1	
9.0	1.0	1.0	31 ± 1	
		benzoate		
9.0	0	1.0	16 ± 1	
9.0	1.0	1.0	34 ± 1	
		ethanol		
9.0	0	1.0	19 ± 1	
9.0	1.0	1.0	31 ± 1	
		tert-butyl alcohol		
9.0	0	1.0	24 ± 2	
9.0	0	2.0	19 ± 1	
9.0	0.50	1.0	31 ± 1	
9.0	0.50	2.0	27 ± 2	

[a] Total peroxynitrite was 0.55 mM. [b] Errors shown are the standard deviation of triplicate measurements. [c] Assuming that $^{\bullet}O_2^- + NO_2^-$ are the products in reaction 3; the alternative pathway gives very similar values.

6, 8, and 10, was equal to the initial amount of added peroxynitrite (data not shown). These observations are in accord with results reported earlier by Mayer, Bohle, and co-workers.[38] Control experiments with peroxynitrite solutions that had been

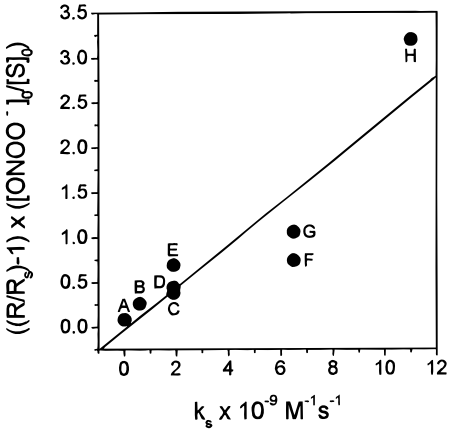

Figure 2. Inhibition of the initial rate of O_2 formation by acetate (A), *tert*-butyl alcohol (B), ethanol (C), mannitol (D), 2-propanol (E), DMSO (F), benzoate (G), and $Fe(CN)_6^{4-}$ (H) in 0.3 M phosphate buffer (pH 9). Each point is the average of 3−6 measurements with 0.5 mM total initial peroxynitrite. Scavenger concentrations (0.5−2.0 mM) were chosen so that inhibition was ∼50% and was linearly dependent upon the scavenger concentration. Rate constants (k_S) for reaction of each scavenger (S) with $^{\bullet}OH$ were taken from ref 39. The line is the linear least-squares fit to the data.

treated with MnO_2 to remove any residual H_2O_2 gave results that were identical with those obtained with untreated samples, thus establishing that oxidation of adventitious H_2O_2 by peroxynitrite was not a source of O_2 in these studies.

Inhibition of O_2 Formation by Radical Scavengers. Oxygen yields from peroxynitrite decomposition decreased upon addition of the $^{\bullet}OH$ scavengers DMSO, benzoate, ethanol, 2-propanol, *tert*-butyl alcohol, acetate, mannitol, or $Fe(CN)_6^{4-}$ to the reaction medium. In neutral solutions, addition of NO_2^-, an efficient $^{\bullet}OH$ scavenger,[39] also inhibited O_2 formation, but this inhibition became progressively less effective as the pH was increased; above pH 9, NO_2^- concentrations as high as 0.4 M had no effect upon the O_2 yields. Furthermore, inhibition of O_2 formation by the organic radical scavengers at pH 9 could be completely reversed by adding NO_2^-. This result is remarkable in light of the absence of any effects of added NO_2^- upon the O_2 yields when other scavengers were not present. Notably, NO_2^- did not reverse the strong inhibition of O_2 formation by $Fe(CN)_6^{4-}$. Data illustrating these effects are presented in Table 1.

Addition of 50 mM bicarbonate to the medium completely blocked O_2 formation. Under the experimental conditions, the concentration of CO_2 derived from bicarbonate was ∼1 mM, ensuring that virtually all of the reaction proceeded via intermediary formation of $ONOOCO_2^-$. As might be expected from the effects of other alcohols, 6% poly(ethylene glycol) (average MW 10 000) also completely inhibited O_2 formation.

Initial rates of O_2 formation at pH 9.0 in the presence of various scavengers are presented in Figure 2 in the form of a competition plot. For simple competition kinetics between a scavenger (S) and $ONOO^-$ for $^{\bullet}OH$, a linear relationship is predicted between k_S (the bimolecular rate constant for reaction of S with $^{\bullet}OH$) and the function,

$$\left(\frac{R}{R_S} - 1\right)\frac{[ONOO^-]_o}{[S]_o}$$

where R_S and R are the initial rates of O_2 formation in the presence and absence of the scavenger, respectively, and the

(39) Buxton, J. V.; Greenstock, C. L.; Helman, W. P.; Ross, A. B. *J. Phys. Chem. Ref. Data* **1988**, *17*, 513−886.

Scheme 2

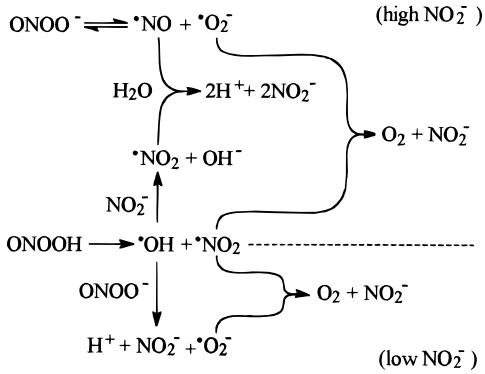

subscripts "o" refer to initial concentrations of the reactant species. Furthermore, the inverse of the slope must be equal to the rate constant for reaction of •OH with $ONOO^-$, i.e.,

$$^{\bullet}OH + ONOO^- \rightarrow H^+ + {}^{\bullet}O_2^- + NO_2^- \quad (\text{or } OH^- + {}^{\bullet}ONOO) \quad (3)$$

The plot of experimental data (Figure 2) is approximately linear and gives a best-fit value of $k_3 = 4 \times 10^9$ M^{-1} s^{-1}, nearly identical with the rate constant ($k_3 = 4.8 \times 10^9$ M^{-1} s^{-1}) measured by pulse radiolysis.[31] Thus, the relative reactivities of the oxidizing intermediate toward the scavengers and peroxynitrite are comparable to those of •OH.

One potential complication not addressed by this analysis involves the fate of secondary radicals formed upon oxidation of the scavengers with the intermediate. Reaction of these radicals with adventitious NO_2^- could cause additional O_2 formation via the intermediacy of $^{\bullet}NO_2$ (see, e.g., Scheme 2). In this case, experimentally measured initial rates of formation and overall O_2 yields would be greater than expected for the simple competition model, leading to underestimation of k_3. For the scavengers NO_2^- and $Fe(CN)_6^{4-}$, sufficient kinetic information exists to calculate their effects on O_2 yields, as described in the following section.

Kinetic Simulations. Yields of O_2 formed under the various reaction conditions were modeled assuming that free radicals are generated by two homolytic decompositions:

$$ONOOH \rightarrow 0.71HNO_3 + 0.29{}^{\bullet}NO_2 + 0.29{}^{\bullet}OH \quad (4)$$

$$ONOO^- \rightleftharpoons {}^{\bullet}NO + {}^{\bullet}O_2^- \quad (5)$$

A radical yield of 29% in reaction 4 is based upon the observed yield of the oxidizing intermediate formed in ONOOH decompositions,[40] for which $k_4 = 0.8$ s^{-1} at the prevailing temperature (~21 °C). The forward rate constant for reaction 5 was recently measured to be $k_5 = 0.017$ s^{-1};[33] for the reverse reaction, we used $k_{-5} = 5 \times 10^9$ M^{-1} s^{-1}, which is the average of two reported values.[41,42] The relative contributions of reactions 4 and 5 to radical generation are determined by the medium pH and the pK_a of ONOOH, which was taken as 6.6.[11]

The hydroxyl radical produced in reaction 4 can react with $ONOO^-$ (reaction 3).[31] The immediate products of this reaction are unknown; the two most probable pathways, comprising either O atom abstraction or electron transfer (reaction 3), were explored in the simulations and gave practically identical oxygen yields under all conditions (Figure 1). Because ab initio calculations[43] have suggested that the electron-transfer product, •ONOO, decomposes to $^{\bullet}NO + O_2$; the electron-transfer pathway was modeled as producing these species directly. Nitrite ion, which is both an unavoidable contaminant in most $ONOO^-$ preparations and a product of the O_2-evolving pathway, reacts rapidly with •OH:

$$^{\bullet}OH + NO_2^- \rightarrow OH^- + {}^{\bullet}NO_2 \quad (6)$$

with $k_6 = 1 \times 10^{10}$ M^{-1} s^{-1}.[39] Other reactions of •OH, e.g., with $^{\bullet}O_2^-$, $^{\bullet}NO_2$, •NO, or •OH, are second order in radicals, and therefore too slow to compete with reactions 3 and 6 under the experimental conditions. Consequently, these reactions were not included in the simulations.

Most of the oxygen is expected to be generated from superoxide radical:

$$^{\bullet}NO_2 + {}^{\bullet}O_2^-(^{\bullet}HO_2) \rightarrow O_2NOO^- \rightarrow NO_2^- + O_2 \quad (7)$$

This reaction is pH dependent ($pK_a(^{\bullet}HO_2) = 4.8$) with reported rate constants[44] of $k_7(^{\bullet}O_2^-) = 4.5 \times 10^9$ M^{-1} s^{-1} and $k_7(^{\bullet}HO_2) = 1.8 \times 10^9$ M^{-1} s^{-1}. Since O_2NOO^- decomposes relatively rapidly[44] ($k = 1$ s^{-1}), reaction 7 was treated as proceeding directly to its final products. Under our experimental conditions, disproportionation of superoxide is too slow[45] to compete with reaction 7; incorporation of the $^{\bullet}O_2^-$ disproportionation step into the simulated mechanism did not alter the calculated yields of O_2.

Radical termination proceeds through a well-established set of reactions:

$$^{\bullet}NO_2 + {}^{\bullet}NO_2 \rightleftharpoons N_2O_4 \quad (8)$$

$$N_2O_4 + H_2O \rightarrow NO_2^- + NO_3^- + 2H^+ \quad (9)$$

$$^{\bullet}NO_2 + {}^{\bullet}NO \rightleftharpoons N_2O_3 \quad (10)$$

$$N_2O_3 + H_2O(OH^-) \rightarrow 2NO_2^- + 2H^+(H^+) \quad (11)$$

for which $k_8 = 4.5 \times 10^8$ M^{-1} s^{-1}, $k_{-8} = 6.9 \times 10^3$ s^{-1}, $k_9 = 1 \times 10^3$ s^{-1}, $k_{10} = 1.1 \times 10^9$ M^{-1} s^{-1}, $k_{-10} = 8.4 \times 10^4$ s^{-1}, $k_{11} = (2 \times 10^3) + (1 \times 10^8[OH^-])$ s^{-1}.[46-48] In addition to hydrolyzing, the electrophilic N_2O_3 intermediate reacts with peroxynitrite anion:

$$N_2O_3 + ONOO^- \rightarrow NO_2^- + 2{}^{\bullet}NO_2 \quad (12)$$

with a rate constant of $k_{12} = 3 \times 10^8$ M^{-1} s^{-1}.[32] In neutral and weakly alkaline solutions, this reaction leads to radical chain propagation that significantly boosts O_2 production by accelerating reaction 7.

The mechanism represented by reactions 3−12 can be quantitatively tested because rate constants for each of the steps have been determined in independent studies. The details of our analysis by numeric integration are given as Supporting

(40) Based upon recent measurements with $Fe(CN)_6^{4-}$ and $IrCl_6^{3-}$ as reductants (Gerasimov, O. V.; Lymar, S. V. Unpublished observations).
(41) Huie, R. E.; Padmaja, S. *Free Radical Res. Commun.* **1993**, *18*, 195−199.
(42) Goldstein, S.; Czapski, G. *Free Radical Biol. Med.* **1995**, *19*, 505−510.
(43) McKee, M. L. *J. Am. Chem. Soc.* **1995**, *117*, 1629−1637.
(44) Logager, T.; Sehsted, K. *J. Phys. Chem.* **1993**, *97*, 10047−10052.
(45) Bielski, B. H.; Cabelli, D. E.; Arudi, R. L. *J. Phys. Chem. Ref. Data* **1985**, *14*, 1041−1100.
(46) Gratzel, M.; Henglein, A.; Lilie, J.; Beck, G. *Ber. Bunsen-Ges. Phys. Chem.* **1969**, *73*, 646−653.
(47) Gratzel, M.; Taniguchi, S.; Henglein, A. *Ber. Bunsen-Ges. Phys. Chem.* **1970**, *74*, 488−492.
(48) Treinin, A.; Hayon, E. *J. Am. Chem. Soc.* **1970**, *92*, 5821−5828.

Information. As shown in Figure 1, calculated O_2 yields based upon this mechanism accurately reproduce measured values over the accessible experimental pH range. The calculated yields for NO_2^- were always twice those for O_2, as expected, because overall stoichiometry of reactions 3−12 is:

$$ONOOH + ONOO^- = 2yO_2 + 4yNO_2^- + (2-4y)NO_3^- + H^+ \quad (13)$$

where $0 \le y \le 0.5$ is the pH-dependent oxygen yield. Because reactions involving nitrite are explicitly included in the mechanism, one can model the effects of deliberately added NO_2^- on the O_2 yields. Comparison with experimental results (Table 1) indicates that our mechanism accounts fairly well for the complex pH-dependent inhibition by NO_2^-. The simulations also predict that O_2 yields will be insensitive to the initial peroxynitrite concentration; the calculated yield decreased by 5% upon lowering $[ONOO^-]_{t=0}$ from 0.55 to 0.14 mM at pH 9. Finally, the inhibition of O_2 formation by $Fe(CN)_6^{4-}$ and its modulation by NO_2^- can be estimated by including in the scheme three additional reactions, i.e.,

$$Fe(CN)_6^{4-} + {}^\bullet OH \rightarrow Fe(CN)_6^{3-} + OH^- \quad (14)$$

$$Fe(CN)_6^{4-} + {}^\bullet NO_2 \rightarrow Fe(CN)_6^{3-} + NO_2^- \quad (15)$$

$${}^\bullet O_2^- + Fe(CN)_6^{3-} \rightarrow O_2 + Fe(CN)_6^{4-} \quad (16)$$

for which $k_{14} = 1.1 \times 10^{10}$ M^{-1} s^{-1}, $k_{15} = 2.1 \times 10^6$ M^{-1} s^{-1}, and $k_{16} = 3 \times 10^2$ M^{-1} s^{-1}.[39,45,49] As experimentally observed (Table 1), the model correctly predicts that NO_2^- will not only be unable to reverse the inhibition by $Fe(CN)_6^{4-}$, but will amplify it.

Discussion

Chemical Reactivity and the •OH Model. All aspects of peroxynitrite decomposition that have been quantitatively examined, including the pH-dependent O_2 yields (Figure 1) and the influence of NO_2^- and free radical scavengers on them (Table 1, Figure 2), are in accord with predictions based upon the assumption that decomposition of ONOOH proceeds through formation of •OH as the oxidizing species. The reaction behavior can be understood qualitatively with the aid of Scheme 2, which incorporates the elementary reaction steps involved in O_2 formation. As additional aids to the following discussion, a tabulation of the reaction steps and the ways in which they sum to give net reaction stoichiometries for the various pathways are attached as Supporting Information. In alkaline solutions, where reaction 4 is rate-limiting, the steady-state concentrations of $^\bullet O_2^-$ and •NO are sufficiently high that $^\bullet NO_2$ partitions between reactions 7, 10, and 11; dimerization/hydrolysis (reactions 8 and 9) contributes very little under these conditions. When the NO_2^- concentration is low (Scheme 2, reactions below the dashed line), •OH preferentially oxidizes $ONOO^-$, producing either O_2 + •NO or $^\bullet O_2^-$ + NO_2^- (reaction 3). In the former case, •NO reacts with the $^\bullet NO_2$ generated by ONOOH peroxo bond homolysis (reaction 4), producing two NO_2^- ions (reactions 10 and 11); in the latter case, $^\bullet O_2^-$ reacts with $^\bullet NO_2$ to form O_2 and NO_2^- (reaction 7). In either case, summation of the appropriate reactions yields the net stoichiometry given by reaction 13 with $y \simeq 0.23$; the simulations show that O_2 yields in excess of this value (Figure 1) are entirely due to radical chain propagation via reactions 5, 7, 10, and 12. The maxima in the simulated curves occur when the rates of reactions 11 and 12 are equal; in more alkaline solution, hydrolysis of N_2O_3 (reaction 11) becomes increasingly important, lowering the O_2 yields. The small differences between two pathways for reaction 3 revealed by the simulations (Figure 1) are due to slightly different contributions from the radical termination and propagation steps (reactions 8−12). Formation of $^\bullet O_2^-$ is, in our opinion, more likely, given the tendency of •OH to abstract O atoms; this pathway is the one depicted in Scheme 2.

At high NO_2^- concentrations (Scheme 2, reactions above the dashed line), •OH is effectively scavenged by NO_2^- (reaction 6). Under these conditions, the only source of O_2 is the $^\bullet O_2^-$ generated by reaction 5. Summing reactions 4−7 and 10−11, one again obtains eq 13 with $y \simeq 0.23$. Consequently, addition of NO_2^- has no effect upon the O_2 yield in alkaline solutions, as was both observed and confirmed by the simulations (Table 1).

In neutral or acidic media, however, $^\bullet O_2^-$ formation from $ONOO^-$ by reactions 3 and 5 becomes rate-limiting, so that now $^\bullet NO_2$ dimerization/hydrolytic disproportionation (reactions 8 and 9) competes with $^\bullet O_2^-$ oxidation, thus lowering the O_2 yields. Under these conditions, addition of NO_2^- enhances this effect by promoting reaction 6 at the expense of reaction 3. Indeed, summation of reactions 4, 6, 8, and 9 shows that, when $^\bullet NO_2$ hydrolysis completely predominates, the yield of O_2 becomes negligible. The pH dependence of the O_2 yield (Figure 1) is determined by the relative rates of reactions 4 and 5. Ignoring reaction 12, one can show that the inflection point corresponds to the pH where the rates of reaction 4 and the forward step of reaction 5 are equal.[33] Using $pK_a(ONOOH) = 6.6$, $k_4 = 0.8$ s^{-1}, and $k_5 = 0.017$ s^{-1}, we calculate pH 7.7 for this point, nearly identical with the apparent experimental value (Figure 1).

Organic •OH scavengers attenuated O_2 yields, most likely by reacting directly with •OH to form secondary radicals. Excepting $Fe(CN)_6^{4-}$, this inhibition was reversed in alkaline media by NO_2^- under conditions where it competed effectively with the scavengers for •OH to generate $^\bullet NO_2$ (reaction 6). As described above, substitution of •OH by $^\bullet NO_2$ in alkaline solution does not inhibit O_2 evolution because it preserves the oxidizing equivalent needed for converting $^\bullet O_2^-$ to O_2. In contrast, the organic •OH scavengers apparently consume the oxidant, thus suppressing formation of O_2. In general, complete inhibition was not achieved, but appeared to approach scavenger-dependent plateau values above scavenger concentrations of ∼20 mM that were 15−35% of the amount of O_2 formed in the absence of the scavenger. The unquenched O_2 most likely was formed by reaction between $^\bullet O_2^-$ generated in reaction 5 with the fraction of $^\bullet NO_2$ formed in reaction 4 that was not consumed by secondary radicals produced in the •OH-scavenging reactions. Quantitative evaluation of this effect was precluded by the absence of information concerning the secondary radicals generated by the scavengers. However, $Fe(CN)_6^{4-}$, which is rapidly oxidized by both •OH and $^\bullet NO_2$, completely quenched O_2 formation at sufficiently high concentrations, as expected. In this case, the inhibition could not be reversed by adding NO_2^- (Table 1) because any $^\bullet NO_2$ formed by reaction with •OH was consumed by $Fe(CN)_6^{4-}$ before it could react with $^\bullet O_2^-$. Similarly, no O_2 was observed in the presence of bicarbonate because under the reaction conditions scavenging of peroxynitrite by CO_2

$$ONOO^- + CO_2 \rightarrow ONOOCO_2^- \rightarrow {}^\bullet NO_2 + {}^\bullet CO_3^- \rightarrow NO_3^- + CO_2 \quad (17)$$

(49) Goldstein, S.; Czapski, G. *J. Am. Chem. Soc.* **1995**, *117*, 12078−12084.

dominates all reactions that could be sources for O_2, including homolysis (reaction 5) and oxidation of $ONOO^-$ by $^•CO_3^-$.[11,16,31]

Other Studies. Several arguments have been raised against the formation of discrete •OH radicals during ONOOH decomposition based upon comparative rate measurements,[21] the pressure dependence of the decomposition kinetics,[50] and viscosity effects.[51] Several groups have reported that studies with spin traps[52] and putative hydroxyl radical scavengers[18,21,53,54] do not show the relative reactivity patterns expected for •OH; other researchers, however, have found reactivities to be consistent with •OH formation.[20,22,55−59] Varying contributions from reactions 6 and 17 arising from contamination by NO_2^- and CO_2 could be major sources of these discrepancies. These reactions, which were not recognized as problematical in many of the earlier studies, significantly modulate the reactivity characteristics of peroxynitrite;[11−13,16,17,19,28] in the studies described herein, for example, CO_2 completely quenched O_2 formation and NO_2^- exhibited a complex pH-dependent quenching pattern (Table 1). Additionally, $^•NO_2$ is invariably produced with •OH (Scheme 2), and its reactions with added trapping agents and radicals derived from them need to be explicitly considered.[16]

Activation volumes reported for ONOOH decomposition have ranged from +1.7 cm^3/mol[51] to +9.6 cm^3/mol[26] under various conditions. We have obtained values for $\Delta V^‡$ that were dependent upon the amount of NO_2^- in the medium, increasing from +6 to +14 cm^3/mol when the NO_2^- content was increased from ~50 μM to 5 mM.[60] It has been argued that low $\Delta V^‡$ values are consistent with an activation step involving intramolecular rearrangement, e.g., cis−trans isomerization, but not with a mechanism involving O−O bond homolysis as the activation step, because reactions initiated by single-bond O−O fissions of peroxo compounds in apolar environments generally have activation volumes of $\Delta V^‡ \simeq +10$ cm^3/mol.[61] This large positive value for $\Delta V^‡$ has been attributed primarily to the rate-retarding effect upon cage escape of the geminate radical pair (k_D in Scheme 1) caused by a pressure-dependent increase in medium viscosity.[62] However, extrapolation to aqueous solutions is questionable because the change in viscosity of water with pressure is very small in the experimental region examined.[61] In any event, the large positive values of $\Delta V^‡$ measured for various indirect reactions of ONOOH appear to be inconsistent with a cis−trans activation step.[60]

The ONOOH decomposition rate was unaffected by increase of the medium viscosity 20-fold, which has been taken as evidence against a free radical mechanism.[51] The additives used were poly(ethylene glycol)s, which our studies have shown effectively scavenge the reactive intermediate (Table 1). As previously noted,[51] under these conditions the reaction given by Scheme 1 will be sensitive to viscosity only if both cage return (k_{-C}) and cage escape (k_D) rate constants are relatively large (optimally, $k_{-C} \gg k_D \gg k_N$). The ability to scavenge only ~29% of the decomposing ONOOH as an oxidizing intermediate implies that $k_N > 2k_D$; estimates for the k_{-C}/k_N ratio based upon experimental data are unavailable. Thus, although observation of a viscosity-dependent reduction in rate constants could be taken as consistent with involvement of discrete •OH and $^•NO_2$ intermediates, the absence of such an effect is not compelling evidence against their participation.

It has been reported[59] that peroxynitrite oxidizes H_2O_2 with evolution of O_2. The reaction is indirect, and has been interpreted as involving rate-limiting formation of an activated intermediate of ONOOH. The O_2 yields were pH-dependent, exhibiting a profile very similar to Figure 1, and competition kinetics with free radical scavengers indicated that the intermediate had a reactivity comparable to that of •OH. These observations can be easily accommodated, at least qualitatively, by including in our mechanism the following elementary step:

$$^•OH + H_2O_2(HO_2^-) \rightarrow H_2O + {}^•O_2^- + H^+$$

for which $k(H_2O_2) = 2.7 \times 10^7$ M^{-1} s^{-1} and $k(HO_2^-) = 7.5 \times 10^9$ M^{-1} s^{-1}.[39] Because this reaction is slow in neutral solutions, large concentrations of H_2O_2 (>0.1 M) were required to saturate the O_2 yields.[59] Under these conditions, despite a pK_a of 11.7 for H_2O_2, sufficient HO_2^- could be present to compete with contaminating NO_2^- (reaction 6) for •OH. Quantitative evaluation of the data would require knowledge of the NO_2^- concentration levels in the $ONOO^-$ reagent solutions.

Finally we note that isotopic exchange of O atoms with H_2O has been reported[63] to accompany decomposition of ONOOH to HNO_3; although the exchange mechanism has not been identified, the results are consistent with formation of radical intermediates.

In summary, the available thermodynamic and kinetic data reported for ONOOH decompositions appear to be consistent with generation of free •OH and $^•NO_2$ as intermediary reactants. Given the complexity of these reactions, devising an alternative mechanism that can account for all experimental observations will be a very challenging endeavor.

Acknowledgment. The authors are grateful to Bryan Shaw at WSU for performing the nitrite/nitrate analyses. This research is supported by the National Institute of Allergy and Infectious Diseases (grant No. AI15834 to J.K.H.) and the U.S. Department of Energy (under contract to Brookhaven National Laboratory DE-AC02-98CH10886 from the Division of Chemical Sciences and EMSP grant No. CH37SP23 to S.V.L. from the Office of Environmental Management).

Supporting Information Available: A tabulation of elementary reactions and their rate constants (Table S1); net reaction stoichiometries based upon their summation for the various reaction pathways (Table S2); details concerning the numerical analyses (Table S3) (PDF). This material is available free of charge via the Internet at http://pubs.acs.org.

JA982887T

(50) Kissner, R.; Nauser, T.; Bugnon, P.; Lye, P. G.; Koppenol, W. H. *Chem. Res. Toxicol*. **1997**, *10*, 1285−1292.
(51) Pryor, W. A.; Jin, X.; Squadrito, G. L. *J. Am. Chem. Soc*. **1996**, *118*, 3125−3128.
(52) Lemercier, J. N.; Squadrito, G. L.; Pryor, W. A. *Arch. Biochem. Biophys*. **1995**, *321*, 31−39.
(53) Kooy, N. W.; Royall, J. A.; Ischiropoulos, H.; Beckman, J. S. *Free Radical Biol. Med*. **1994**, *16*, 149−156.
(54) Moreno, J. J.; Pryor, W. A. *Chem. Res. Toxicol.* **1992**, *5*, 425−431.
(55) van der Vliet, A.; O'Neill, C. A.; Halliwell, B.; Cross, C. E.; Kaur, H. *FEBS Lett*. **1994**, *339*, 89−92.
(56) Agusto, O.; Gatti, R.; Radi, R. *Arch. Biochem. Biophys.* **1994**, *310*, 118−125.
(57) Agusto, O.; Radi, R.; Gatti, R. M.; Vasquez-Vivar, J. *Method Enzymol*. **1996**, *269*, 346−354.
(58) Mahoney, L. R. *J. Am. Chem. Soc*. **1970**, *92*, 5262−5263.
(59) Alvarez, B.; Denicola, A.; Radi, R. *Chem. Res. Toxicol*. **1995**, *8*, 859−869.
(60) Coddington, J. W.; Wherland, S.; Hurst, J. K. **1999**, manuscript submitted for publication.
(61) Isaacs, N. S. *Liquid-Phase High-Pressure Chemistry*; Wiley: New York, 1981.
(62) Neuman, R. C., Jr.; Bussey, R. J. *J. Am. Chem. Soc*. **1970**, *92*, 2440−2445.
(63) Bohle, D. S.; Hansert, B. *Nitric Oxide* **1997**, *1*, 502−506.